ICASSP 2025 - 2025 IEEE International Conference on Acoustics, Speech and Signal Processing (ICASSP) | 979-8-3503-6874-1/25/$31.00 ©2025 IEEE | DOI: 10.1109/ICASSP49660.2025.10890136

A Fuzzy C-Means Clustering Algorithm for Real Medical Image Segmentation*

Feifei Zhang[1,2], Fei Shi[1,2,*], Dayong Ren[3,*], and Yue Li[1,2]
[1] Xinjiang University, School of Computer Science and Technology, Xinjiang Urumqi 830046, China.
[2] Xinjiang University, Key Laboratory of Signal Detection and Processing, Xinjiang Urumqi 830046, China.
[3] National Key Laboratory for Novel Software Technology, Nanjing University, Nanjing 210023, China.

***Abstract*—In the field of medical image processing, the presence of noise can often result in the obfuscation of crucial details, which in turn can have a detrimental impact on the accuracy of clinical diagnoses. In order to effectively remove noise and improve segmentation performance, this paper proposes a refined Fuzzy C-Means (FCM) algorithm, designated as MKL-FCM. The method commences with Poisson denoising, which enables more effective handling of the noise characteristics inherent to medical images. Subsequently, multi-scale Kullback-Leibler divergence is utilised to analyse local image information across varying scales, facilitating the differentiation between tissues and pathological regions. Furthermore, tight wavelet frames are capable of capturing fine image details, while reverse optimisation of the objective function serves to correct errors in feature reconstruction, thereby enhancing the accuracy of the segmentation process. The experimental results demonstrate that MKL-FCM enhances both image clarity and segmentation accuracy, and outperforms existing methods in terms of efficiency.**

***Index Terms*—Fuzzy C-means (FCM), multi-scale Kullback-Leibler divergence, Poisson denoising (PD), medical image.**

I. Introduction

In the field of medical image processing, the ability to produce high-quality images is of paramount importance to ensure accurate diagnosis by medical professionals [1]. However, medical images are frequently corrupted by noise introduced by imaging sensors and environmental factors, including Poisson noise, Gaussian noise, and impulse noise [2]. The presence of noise in medical images can result in the obfuscation of critical details, which may ultimately compromise diagnostic accuracy and potentially lead to false positive or missed diagnosis outcomes [3]. This phenomenon can be likened to viewing a landscape through a dust-covered window, where while the general outline remains visible, crucial details are obscured. Consequently, the removal of such noise represents a pivotal step in the processing of medical images, significantly enhancing the accuracy of subsequent segmentation and detection tasks [4]–[10].

The majority of contemporary medical image denoising techniques are predicated on the assumption that noise can be modelled as zero-mean additive Gaussian noise [11], [12]. However, this assumption does not hold for all medical imaging scenarios. In reality, sensor noise in medical images is proportional to the signal intensity, making Poisson noise modelling a more appropriate approach [13], [14]. Under this more realistic assumption, existing methods [14]–[19] have been shown to effectively remove noise while preserving critical image information. This enables doctors to observe image details more clearly, leading to more accurate diagnoses.

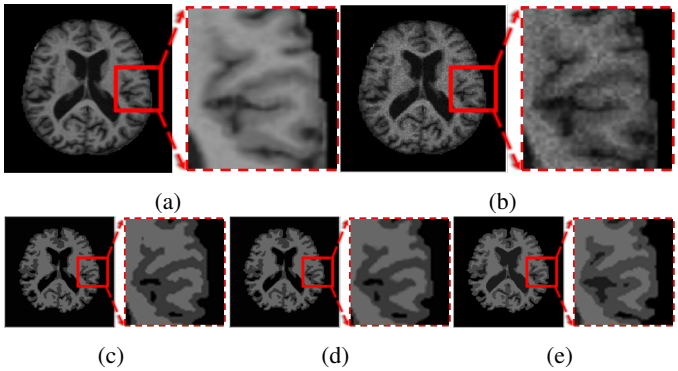

Fig. 1: MKL-FCM Segmentation Process Diagram. (a) Original image. (b) Observed image. (c) Image segmented by MKL-FCM. (d) Reconstructed image. (e) Modified image.

However, the process of image processing does not end with the removal of noise; the subsequent challenge is the accurate segmentation of different tissues and pathological regions within the images. Fuzzy C-Means (FCM) clustering is a commonly used method for image segmentation [20], which has been demonstrated to lack robustness and to produce suboptimal results when dealing with complex, noisy data. As a result, it is insufficient to meet the high precision demands of medical imaging. In recent years, numerous improvements have been proposed by researchers in order to overcome the limitations of the FCM algorithm in handling complex data. Methods such as FCM_S [21], FCM_S1, FCM_S2 [22] and EnFCM [23] have been developed to enhance noise resistance, but they often come with significant computational costs. In order to achieve an optimal balance between segmentation accuracy and computational efficiency, the FCM algorithm has been enhanced through the incorporation of Kullback-Leibler (KL) divergence. Gharieb et al. put forth a KL divergence-based FCM algorithm that optimises the similarity of membership degrees between pixels and their neighbours, thereby markedly enhancing both robustness and computational speed [24]. Lei

* Corresponding author. This work was supported by Tianshan Talent Training Project - Xinjiang Science and Technology Innovation Team Program (2023TSYCTD0012), National Natural Science Foundation of China (No.62261053).

et al. developed the FRFCM algorithm [25], which combines morphological grey-scale reconstruction and membership degree filtering, thereby further enhancing both efficiency and robustness. Wang et al. introduced the KLDFCM algorithm [26], which integrates KL divergence with tight wavelet frame transforms [27], thereby eliminating the need for iterative computation in traditional FCM and greatly improving both segmentation efficiency and robustness.

To combine the advantages of deep learning denoising with the efficiency and robustness of traditional FCM, this paper proposes an improved FCM algorithm based on multi-scale KL divergence for medical image segmentation. As shown in Fig. 2, the method begins with Poisson denoising to reduce noise while preserving critical image details. The use of KL divergence allows the algorithm to capture local information across different scales, improving the accuracy of region delineation. The multi-scale approach processes images at various resolutions, capturing fine tissue differences. By combining advanced noise modeling with the multi-scale KL-based FCM, the algorithm enhances image clarity and highlights key regions, significantly improving segmentation accuracy and efficiency. This approach offers a powerful tool for medical image analysis, contributing to better diagnostic precision and clinical decision-making.

Our contributions to medical imaging with the FCM algorithm focus on three key innovations:

1) We introduce the MKL-FCM algorithm, which incorporates a multi-scale KL divergence term into the FCM objective function, specifically designed for medical images. This approach optimizes high-value target regions by refining the segmentation through scale variations.
2) Given the Poisson noise characteristics in real medical images, we revised the existing noise assumptions and developed a Poisson denoising-based approach.
3) By combining the deep learning-based Poisson denoising approach with the traditional FCM clustering method, the MKL-FCM algorithm significantly improves segmentation accuracy and overall image quality.

II. METHOD

A. Poisson denoising

Our study introduces a cutting-edge Poisson denoising (PD) [14] method for medical images, that overcomes the limitations of traditional models which inaccurately assume noise to be independent of the signal. This method integrates sparse representation, dictionary learning, and self-supervised learning, thus removing the need for clean ground-truth data. Using the repetitiveness of patches in the image and the learnable dictionary D, and applying Convolutional Sparse Coding (CSC) to perform denoising and restore the clean image. This approach outperforms other filtering methods in medical image processing (Figure 3).

We model the pixel values of the noisy image x_0 as Poisson distributed, $x_0[i] \sim \mathcal{P}(\lambda[i])$, and estimate the denoised clean image $x$by maximizing its log-likelihood. To enhance the stability of the optimization, we introduce a sparse representation

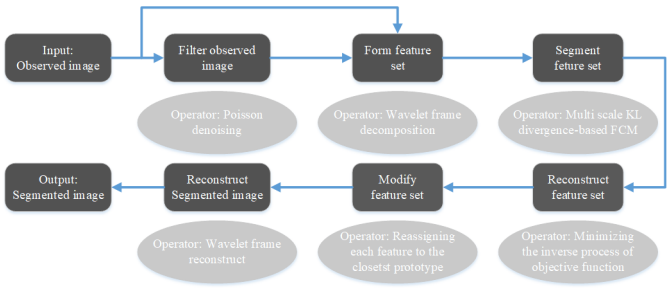

Fig. 2: Framework of the proposed algorithm.

$D\alpha \approx x_0$, and solve the problem through dictionary learning as follows:

$$\min_{D^\top \alpha = x_0, \|\alpha\|_0 \le s, D^\top \alpha \ge 0} \|\alpha\|_1, \tag{1}$$

this optimization problem in Eq. 1 is further relaxed by setting $D\alpha = \exp(D\alpha)$ to handle the non-negativity constraint. Inspired from the Iterative Shrinkage Thresholding Algorithm (ISTA), we propose to solve for α and D in an alternating manner using a neural network-based approach. The ISTA algorithm iteratively refines α in Eq. 1 through $\alpha \leftarrow S(\alpha + \frac{1}{L} D^T(x - D\alpha))$, with $L \le \max(D^T D)$ and $S(z) = \text{sign}(z)\max(|z| - \epsilon, 0)$. To accommodate image dimensions d, we utilize Convolutional Sparse Coding, replacing matrix-vector operations with convolutions $(*)$, making D adapt to image size as $D \in \mathbb{R}^{d \times k}$:

$$D\alpha = \sum_{j=1}^{M} D_j * A_j = D * \mathbf{A}, \tag{2}$$

To use ISTA, we utilize a neural network f_θ to model $D\mathbf{A}$, where f_θ embodies an encoder-decoder structure for calculating sparse representation $\mathbf{A}$, enabling dictionary learning D via back-propagation. This is expressed as $D\mathbf{A} = f_\theta(X_0)$, reformulating Eq. 2 to implicitly promote sparsity within the network framework,

$$\min_\theta \left(\exp(f_\theta(X_0)) - X_0 \odot f_\theta(X_0)\right), \tag{3}$$

where X_0 represents the matrix form of the noisy image x_0, $\odot$ represents the Hadamard product. Moving forward, we denote this as $\mathcal{L}_{\text{Poisson}}$. Drawing on internal learning concepts, our goal is to employ network f_θ to intrinsically impose sparsity via its architecture. We adapt internal learning through the ISTA algorithm, where prior research shows the ISTA update step can be approximated by substituting D and D^T with a decoder and encoder, respectively, in Eq. 2.

$$\mathbf{A} \leftarrow S\left(\mathbf{A} + \text{Encoder}(X_0 - \text{Decoder}(\mathbf{A}))\right), \tag{4}$$

where, S represents the soft-thresholding method. The update in Eq. 4 adopts an RNN-like approach, iteratively refining the sparse code $\mathbf{A}$ over T steps, diverging from traditional sequence processing. This method applies the dictionary to $\mathbf{A}$ within the forward pass, methodically enhancing $\mathbf{A}$ through a predetermined number of iterations, moving away from the conventional convergence-centric ISTA.

B. Multi-scale Kullback-Leibler (KL) divergence-based Fuzzy C-Means (FCM)

In the process of medical image analysis, it is essential to distinguish between background regions (non-informative peripheral areas) and target regions (valuable organs). We argue that optimizing both background and target regions within the same scale may not be ideal. Therefore, we propose a Multi-scale Kullback-Leibler (KL) divergence-based Fuzzy C-Means (FCM) approach. This method is designed to segment background and target regions separately based on the boundary information extracted from medical images.

By introducing spatial information and tight wavelet frames, FCM becomes more robust to noise. We reformulate feature sets associated with f and $\hat{f}$ as $X = \Psi f = \{x_j : j = 1, 2, \ldots, K\}$ and $\hat{X} = \Psi \hat{f} = \{\hat{x}_j : j = 1, 2, \ldots, K\}$. In fact, membership grades of a specific image pixel are close to those of its neighborhoods. Hence, optimizing FCM's partition matrix in each iteration has a positive impact on FCM's segmentation performance. In this article, we use a KL divergence distance D_{KL} to characterize the difference of membership partition between a target pixel x_j and its neighborhoods. Clearly, the distance $D_{KL}(u_{ij}, \hat{u}_{ij})$ should approximate to zero, that is, $D_{KL}(u_{ij}, \hat{u}_{ij}) \to 0$, where u_{ij} is a membership grade stating that x_j belongs to the ith cluster, and $\hat{u}_{ij}$ stands for a median value of membership grades stating that neighborhoods of x_j belong to the ith cluster. Therefore, we can impose a constraint on FCM's objective function as follows:

$$J(U, V) = \sum_{i=1}^{c} \sum_{j=1}^{K} u_{ij} \left(|x_j - v_i|^2 + \alpha |x_j - v_i|^2 \right), \tag{5}$$

$$D_{KL}(U, \hat{U}) = \sum_{i=1}^{c} \sum_{j=1}^{K} u_{ij} \log \frac{u_{ij}}{\hat{u}_{ij}} = 0, \tag{6}$$

where α is a positive parameter that controls the impact of a filtered term $\|\hat{x}_j - v_i\|^2$ on FCM. The entire image is divided into background and target regions based on the pre-segmentation scheme (OTSU) [28], with the optimization process focusing primarily on the target region. Hence, the final formulation of the KLDFCM is:

$$\begin{aligned} J(U, V) = & \sum_{n=1}^{2} \sum_{i=1}^{c} \sum_{j=1}^{K} u_{ij} \left(|x_j - v_i|^2 + \alpha |\hat{x}_j - v_i|^2 \right) \\ & + \beta \sum_{n=1}^{2} \sum_{i=1}^{c} \sum_{j=1}^{K} u_{ij} \log \frac{u_{ij}}{\hat{u}_{ij}}, \end{aligned} \tag{7}$$

where β is a positive parameter that controls the impact of the KL divergence term $D_{KL}(U, \hat{U})$ on FCM. The fuzzification exponent m is not present in Eq. 7. The KL divergence term $D_{KL}(U, \hat{U})$ involves an original partition matrix $U = [u_{ij}]_{c \times K}$ and a filtered partition matrix $\hat{U} = [\hat{u}_{ij}]_{c \times K}$ that is

$$\hat{U} = \mathrm{PD}(U). \tag{8}$$

Here, PD refers to the Poisson denoising method for medical images. In Eq. 6, KL divergence is first introduced into FCM's objective function. Unlike our approach, mean filtering is used to construct the KL divergence term, which performs worse than median filtering in experiments. Additionally, [25] highlights two issues: 1) KL divergence increases computational complexity, and 2) it lacks a robust kernel distance. Our work addresses these shortcomings using PD and tight wavelet frames. We apply the Lagrange multiplier method to minimize Eq. 7. The iterative updates of the partition matrix U and prototypes v_i are given as follows:

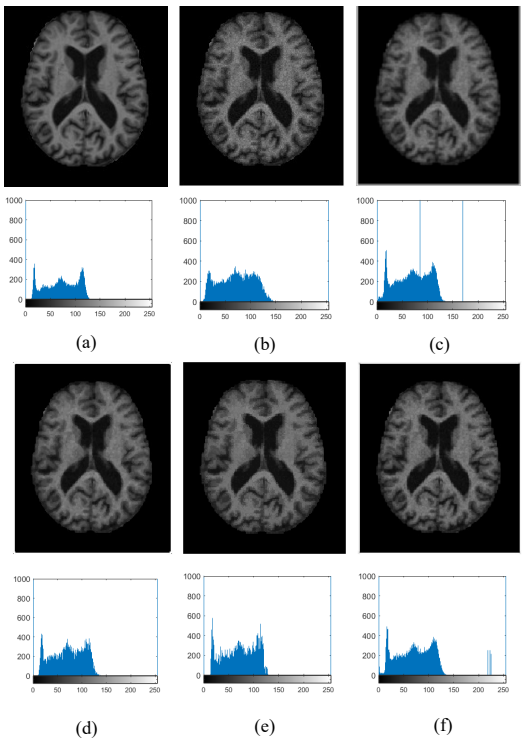

Fig. 3: Comparison with different filtering methods. (a) Original image. (b) Observed image. (c) Result using mean filter. (d) Result using median filter. (e) Result using morphological filter. (f) Result using Poisson denoising.

$$u_{ij} = \frac{\tilde{u}_{ij} e^{-\left(\|x_j - v_i\|^2 + \alpha \|x_j - \tilde{v}_i\|^2 \right)/\beta}}{\sum_{q=1}^{c} \tilde{u}_{qj} e^{-(\|x_j - v_q\|^2 + \alpha \|x_j - \tilde{v}_q\|^2)/\beta}} \tag{9}$$

$$v_i = \frac{\sum_{j=1}^{K} u_{ij} (x_j + \alpha x_j)}{(1 + \alpha) \sum_{j=1}^{K} u_{ij}}. \tag{10}$$

III. Experiments and Results

In this section, we conduct a series of numerical experiments to validate the effectiveness and efficiency of the proposed algorithm. We provide a report on the segmentation results of MKL-FCM on medical images. Simultaneously, we compare the MKL-FCM algorithm with five existing algorithms, including FGFCM [29] and its variants FGFCM_S1 and FGFCM_S2, FRFCM [24], and KLDFCM [26]. In addition to subjective comparisons, this study employs four objective evaluation metrics for a quantitative comparison of our proposed method: 1) SA; 2) Sensitivity (Sen); 3) 95% Hausdorff

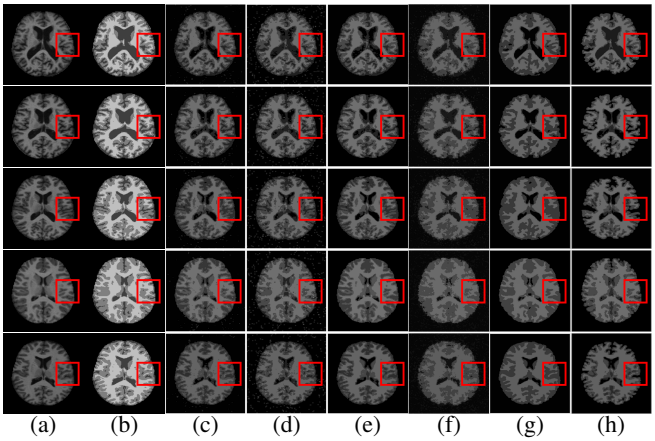

(a) (b) (c) (d) (e) (f) (g) (h)

Fig. 4: Segmentation results on medical images. (a) noisy images. (b) ground truth. (c)FGFCM. (d) FGFCM_S1. (e) FGFCM_S2. (f) LRFCM. (g) KLDFCM. (h) MKL-FCM.

Distance (HD95) and 4) Partition Coefficient (PC) [26]. All experiments in this paper were conducted on a CPU laptop equipped with an 11th Gen Intel(R) Core(TM) i5-11400H @ 2.70GHz and 60.0 GB RAM within MATLAB R2019a.

A. Parameter Setting and Dataset

The parameters used in this study's algorithm were adopted from those selected for the KLDFCM algorithm [26], including a 3×3 local window and a fuzziness index set to $m = 2$. Notably, the algorithm in this paper and KLDFCM do not involve the fuzziness index. Additionally, a threshold value of $\varepsilon = 1 \times 10^{-6}$ was set in all algorithms, assuming that the number of clusters c is known and set to the same value for all algorithms. Other parameters were adopted as recommended by KLDFCM [26] and as set in the original paper. Moreover, based on empirical evidence, the parameters α and β were chosen as 5.5 and 2000, respectively. The OASIS-1 dataset [30] , comprises T1-weighted magnetic resonance imaging (MRI) scans from 421 subjects, aged between 18 and 96 years. The scans have a resolution of (176×208 pixels, with a slice thickness of 1.25mm, which provides labels for cerebrospinal fluid (CSF), grey matter (GM), and white matter (WM).

B. Results for Medical Images

We apply MKL-FCM to the MRI axial images presented earlier. Fig. 4 provides a subjective comparison of segmentation results for five MRI images, with the number of clusters set to 4. The MKL-FCM effectively preserves image details while emphasizing changes in MRI edges. Objective comparison results are summarized in Table I, where the MKL-FCM algorithm demonstrates superior outcomes. Combining subjective and objective evaluations, MKL-FCM proves to be effective in medical image segmentation.

C. Ablation Studies and Analysis

This paper introduces two key components: 1) Image Denoising and 2) Multi-Scale Kullback-Leibler (KL) Divergence.

TABLE I: Average Scores of Segmentation Results.

Method	SA(↑)	PC(↑)	Sen (↑)	HD95(↓)
FGFCM	0.8380	0.8644	0.8553	8.1176
FGFCM_S1	0.8333	0.8969	0.8446	8.2277
FGFCM_S2	0.8395	0.8841	0.8604	8.1057
LRFCM	0.8398	0.8764	0.8455	8.1257
KLDFCM	0.8248	**0.9745**	0.7876	8.2054
MKL-FCM	**0.8545**	0.9553	**0.9049**	**7.5784**

We conduct an ablation study to compare these components' effects. Random Poisson noise is applied to images (Fig. 3b), and the outcomes of mean filter, median filter, morphological filter, and the proposed Poisson denoising are compared, demonstrating the superiority of the proposed approach. Experimental parameters $\boldsymbol{\alpha}$ are set to 5.5 and $\boldsymbol{\beta}$ to 2000, while other parameters match those chosen in KLDFCM [26]. Table II presents the results, with ✓ indicating the component's use and ✗ indicating its absence.

TABLE II: Study of Key Components in the MKL-FCM Algorithm.

Poisson Denoising	M-KL	SA ↑	PC ↑
✗	✗	0.8152	0.9741
✓	✗	0.81815	**0.9743**
✗	✓	0.83957	0.9576
✓	✓	**0.8545**	0.9553

In the absence of the denoising component and the Multi-Scale KL Divergence (MKL) module, the algorithm attains an SA of 0.8152 and a PC of 0.9741. In the absence of the denoising component and the use of MKL alone, the SA reaches 0.83957, while the PC is 0.9576. Conversely, in the absence of MKL and with the denoising component, the SA and PC are 0.81815 and 0.9743, respectively. The presence of both components resulted in an SA of 0.92802, while the PC remained high at 0.9553. Although the application of MKL in isolation results in a reduction in the PC, the concurrent utilisation of both components markedly enhances the algorithm's SA.

IV. Conclusion

We present MKL-FCM, which addresses limitations of the traditional Fuzzy C-Means (FCM) algorithm with noisy images. This Multi-Scale Kullback-Leibler (KL) Divergence-based algorithm enhances FCM by integrating spatial information, kernel distances, and Poisson denoising, significantly improving its robustness. A key advancement is the incorporation of multi-scale KL divergence into FCM's objective function, optimizing membership partitioning for pre-segmented medical images and enhancing pixel membership cohesion. Poisson denoising effectively mitigates noise in real medical images, augmenting FCM's capabilities.

V. Compliance with Ethical Standards

This research study was conducted retrospectively using human subject data made available in open access by OASIS-1 dataset. Ethical approval was not required as confirmed by the license attached with the open access data

REFERENCES

[1] Jingyu Xu, Binbin Wu, Jiaxin Huang, Yulu Gong, Yifan Zhang, and Bo Liu, "Practical applications of advanced cloud services and generative ai systems in medical image analysis," *arXiv preprint arXiv:2403.17549*, 2024.

[2] Zhaolin Chen, Kamlesh Pawar, Mevan Ekanayake, Cameron Pain, Shenjun Zhong, and Gary F Egan, "Deep learning for image enhancement and correction in magnetic resonance imaging—state-of-the-art and challenges," *Journal of Digital Imaging*, vol. 36, no. 1, pp. 204–230, 2023.

[3] Subrato Bharati, Tanvir Zaman Khan, Prajoy Podder, and Nguyen Quoc Hung, "A comparative analysis of image denoising problem: noise models, denoising filters and applications," *Cognitive Internet of Medical Things for Smart Healthcare: Services and Applications*, pp. 49–66, 2021.

[4] Dayong Ren, Zhengyi Wu, Jiawei Li, Piaopiao Yu, Jie Guo, Mingqiang Wei, and Yanwen Guo, "Point attention network for point cloud semantic segmentation," *Science China Information Sciences*, vol. 65, no. 9, pp. 192104, 2022.

[5] Dayong Ren, Zhe Ma, Yuanpei Chen, Weihang Peng, Xiaode Liu, Yuhan Zhang, and Yufei Guo, "Spiking pointnet: Spiking neural networks for point clouds," *Advances in Neural Information Processing Systems*, vol. 36, 2024.

[6] Dayong Ren, Jiawei Li, Zhengyi Wu, Jie Guo, Mingqiang Wei, and Yanwen Guo, "Mffnet: multimodal feature fusion network for point cloud semantic segmentation," *The Visual Computer*, vol. 40, no. 8, pp. 5155–5167, 2024.

[7] Yanwen Guo, Yuanqi Li, Dayong Ren, Xiaohong Zhang, Jiawei Li, Liang Pu, Changfeng Ma, Xiaoyu Zhan, Jie Guo, Mingqiang Wei, et al., "Lidar-net: A real-scanned 3d point cloud dataset for indoor scenes," in *Proceedings of the IEEE/CVF Conference on Computer Vision and Pattern Recognition*, 2024, pp. 21989–21999.

[8] Chen Chen, Yisen Wang, Honghua Chen, Xuefeng Yan, Dayong Ren, Yanwen Guo, Haoran Xie, Fu Lee Wang, and Mingqiang Wei, "Geosegnet: point cloud semantic segmentation via geometric encoder–decoder modeling," *The Visual Computer*, vol. 40, no. 8, pp. 5107–5121, 2024.

[9] Dayong Ren, Shuangyu Yang, WEN JIE LI, Jie Guo, and Yanwen Guo, "Sae: Estimation for transition matrix in annotation algorithms," .

[10] Feifei Zhang, Fei Shi, Dayong Ren, Zhenhong Jia, and Jianyi Wang, "Dual-mambanet: A lightweight dual-branch brain image segmentation network based on local attention and mamba," in *International Conference on Pattern Recognition*. Springer, 2024, pp. 92–107.

[11] Liangyu Chen, Xin Lu, Jie Zhang, Xiaojie Chu, and Chengpeng Chen, "Hinet: Half instance normalization network for image restoration," in *Proceedings of the IEEE/CVF conference on computer vision and pattern recognition*, 2021, pp. 182–192.

[12] Syed Waqas Zamir, Aditya Arora, Salman Khan, Munawar Hayat, Fahad Shahbaz Khan, Ming-Hsuan Yang, and Ling Shao, "Multi-stage progressive image restoration," in *Proceedings of the IEEE/CVF conference on computer vision and pattern recognition*, 2021, pp. 14821–14831.

[13] Samuel W Hasinoff, "Photon, poisson noise," in *Computer vision: a reference guide*, pp. 980–982. Springer, 2021.

[14] Calvin-Khang Ta, Abhishek Aich, Akash Gupta, and Amit K Roy-Chowdhury, "Poisson2sparse: Self-supervised poisson denoising from a single image," in *International Conference on Medical Image Computing and Computer-Assisted Intervention*. Springer, 2022, pp. 557–567.

[15] James Pawley, "Fundamental limits in confocal microscopy," in *Handbook of biological confocal microscopy*, pp. 15–26. Springer, 2006.

[16] Lucas Sjulson and Gero Miesenbock, "Optical recording of action potentials and other discrete physiological events: a perspective from signal detection theory," *Physiology*, vol. 22, no. 1, pp. 47–55, 2007.

[17] Abd-Krim Seghouane, Asif Iqbal, and Aref Miri Rekavandi, "Rbdl: Robust block-structured dictionary learning for block sparse representation," *Pattern Recognition Letters*, vol. 172, pp. 89–96, 2023.

[18] Aref Miri Rekavandi, Abd-Krim Seghouane, and Karim Abed-Meraim, "Trpast: A tunable and robust projection approximation subspace tracking method," *IEEE Transactions on Signal Processing*, vol. 71, pp. 2407–2419, 2023.

[19] Aref Miri Rekavandi, Abd-Krim Seghouane, and Robin J Evans, "Learning robust and sparse principal components with the α-divergence," *IEEE Transactions on Image Processing*, 2024.

[20] Zhenhua Shi, Dongrui Wu, Chenfeng Guo, Changming Zhao, Yuqi Cui, and Fei-Yue Wang, "Fcm-rdpa: Tsk fuzzy regression model construction using fuzzy c-means clustering, regularization, droprule, and powerball adabelief," *Information Sciences*, vol. 574, pp. 490–504, 2021.

[21] Mohamed N Ahmed, Sameh M Yamany, Nevin Mohamed, Aly A Farag, and Thomas Moriarty, "A modified fuzzy c-means algorithm for bias field estimation and segmentation of mri data," *IEEE transactions on medical imaging*, vol. 21, no. 3, pp. 193–199, 2002.

[22] Songcan Chen and Daoqiang Zhang, "Robust image segmentation using fcm with spatial constraints based on new kernel-induced distance measure," *IEEE Transactions on Systems, Man, and Cybernetics, Part B (Cybernetics)*, vol. 34, no. 4, pp. 1907–1916, 2004.

[23] László Szilagyi, Zoltán Benyo, Sándor M Szilágyi, and HS Adam, "Mr brain image segmentation using an enhanced fuzzy c-means algorithm," in *Proceedings of the 25th annual international conference of the IEEE engineering in medicine and biology society (IEEE Cat. No. 03CH37439)*. IEEE, 2003, vol. 1, pp. 724–726.

[24] Reda Ragab Gharieb, G Gendy, A Abdelfattah, and Hany Selim, "Adaptive local data and membership based kl divergence incorporating c-means algorithm for fuzzy image segmentation," *Applied Soft Computing*, vol. 59, pp. 143–152, 2017.

[25] Tao Lei, Xiaohong Jia, Yanning Zhang, Lifeng He, Hongying Meng, and Asoke K Nandi, "Significantly fast and robust fuzzy c-means clustering algorithm based on morphological reconstruction and membership filtering," *IEEE Transactions on Fuzzy Systems*, vol. 26, no. 5, pp. 3027–3041, 2018.

[26] Cong Wang, Witold Pedrycz, ZhiWu Li, and MengChu Zhou, "Kullback–leibler divergence-based fuzzy c-means clustering incorporating morphological reconstruction and wavelet frames for image segmentation," *IEEE Transactions on cybernetics*, vol. 52, no. 8, pp. 7612–7623, 2021.

[27] Cong Wang, Witold Pedrycz, MengChu Zhou, and ZhiWu Li, "Sparse regularization-based fuzzy c-means clustering incorporating morphological grayscale reconstruction and wavelet frames," *IEEE Transactions on Fuzzy Systems*, vol. 29, no. 7, pp. 1826–1840, 2020.

[28] Ta Yang Goh, Shafriza Nisha Basah, Haniza Yazid, Muhammad Juhairi Aziz Safar, and Fathinul Syahir Ahmad Saad, "Performance analysis of image thresholding: Otsu technique," *Measurement*, vol. 114, pp. 298–307, 2018.

[29] Weiling Cai, Songcan Chen, and Daoqiang Zhang, "Fast and robust fuzzy c-means clustering algorithms incorporating local information for image segmentation," *Pattern recognition*, vol. 40, no. 3, pp. 825–838, 2007.

[30] Daniel S Marcus, Tracy H Wang, Jamie Parker, John G Csernansky, John C Morris, and Randy L Buckner, "Open access series of imaging studies (oasis): cross-sectional mri data in young, middle aged, nondemented, and demented older adults," *Journal of cognitive neuroscience*, vol. 19, no. 9, pp. 1498–1507, 2007.